

Connecting the LHC diphoton excess to the Galactic center gamma-ray excess

Xian-Jun Huang, Wei-Hong Zhang, Yu-Feng Zhou *

*Key Laboratory of Theoretical Physics,
Institute of Theoretical Physics, Chinese Academy of Sciences
ZhongGuanCun East Rd.55, Beijing, 100190, China
School of Physical Sciences, University of Chinese Academy of Sciences
Yuquan Rd.19A, Beijing 100049, China*

Abstract

The recent LHC Run-2 data have shown a possible excess in diphoton events, suggesting the existence of a new resonance ϕ with mass $M \sim 750$ GeV. If ϕ plays the role of a portal particle connecting the Standard Model and the invisible dark sector, the diphoton excess should be correlated with another photon excess, namely, the excess in the diffuse gamma rays towards the Galactic center, which can be interpreted by the annihilation of dark matter (DM). We investigate the necessary conditions for a consistent explanation for the two photon excesses, especially the requirement on the width-to-mass ratio Γ/M and ϕ decay channels, in a collection of DM models where the DM particle can be scalar, fermionic and vector, and ϕ can be generated through s -channel gg fusion or $q\bar{q}$ annihilation. We show that the minimally required Γ/M is determined by a single parameter proportional to $(m_\chi/M)^n$, where the integer n depends on the nature of the DM particle. We find that for the scalar DM model with ϕ generated from $q\bar{q}$ annihilation, the minimally required Γ/M can be as low as $\mathcal{O}(10^{-3})$. For the scalar DM model with ϕ generated from gg fusion and fermionic DM model with ϕ from $q\bar{q}$ annihilation, the required Γ/M are typically of $\mathcal{O}(10^{-2})$. The vector DM models, however, require very large Γ/M of order one. For the DM models which can consistently explain both the excesses, the predicted cross sections for gamma-ray line are typically of $\mathcal{O}(10^{-31} - 10^{-29}) \text{ cm}^3\text{s}^{-1}$, which are close to the current limits from the Fermi-LAT experiment.

*Email: huangxj@itp.ac.cn, whzhang@itp.ac.cn, yfzhou@itp.ac.cn

1 Introduction

Recently, the ATLAS and CMS collaborations have reported the results of the LHC Run-2 at center-of-mass energy $\sqrt{s} = 13$ TeV, based on the integrated luminosity of 3.2 fb^{-1} and 3.3 fb^{-1} , respectively [1]. Both the collaborations have shown a possible excess in the events containing two photons, suggesting the existence of a new s -channel resonance particle ϕ . The distribution of the observed events at ATLAS favours a mass of the resonance $M \approx 750$ GeV, and a width-to-mass ratio $\Gamma/M \approx 0.06$ with a local (global) significance of 3.9σ (2.3σ). In the assumption of a narrow width, the corresponding local (global) significance is 3.6σ (2.0σ). The CMS collaboration has also reported a similar excess at $M \approx 760$ GeV with a local (global) significance of 2.9σ ($< 1\sigma$), and the event distribution slightly favours a narrow width. A combined analysis of the CMS Run-1 (8 TeV) and Run-2 data showed that the local (global) significance of the diphoton excess increases to 3.4σ (1.6σ) with the best-fit diphoton invariant mass close to 750 GeV [2]. If the two photons arise directly from the decay of the resonance ϕ , the resonance must be electrically neutral, and its spin can be 0 or 2 due to the Landau-Yang theorem [3]. Assuming a large width, the ATLAS (CMS) data favour a diphoton production cross section $10 \pm 3 \text{ fb}$ ($6 \pm 3 \text{ fb}$) [4]. Other analyses assuming narrow width give ~ 6.2 (5.6) fb for ATLAS (CMS) [5, 6].

The LHC diphoton excess, if confirmed, is a clear indication of new physics beyond the standard model (SM). Furthermore, ϕ is unlikely to be the only new particle. Since ϕ is electrically neutral, it can only couple to photons through loop processes. If the loops involve only the SM charged particles, ϕ should decay into these SM particles with large rates, as ϕ is much heavier than all the SM particles. The corresponding production cross sections can easily reach $\mathcal{O}(\text{pb})$ which are too large to escape the detection at LHC Run-1 (see e.g. [7, 8]). If the large width $\Gamma/M \approx 0.06$ favoured by ATLAS is confirmed, the resonance ϕ is likely to have additional tree-level invisible decays. An intriguing possibility is that ϕ also couples to the dark matter (DM) particles which contribute to $\sim 26.8\%$ of the energy budget of our Universe. In this scenario, ϕ plays the role of a portal connecting the invisible and visible world. The excess of diphoton events suggests that the DM particle should at least couple to photons, and also couple to gluons or quarks depending on the production mechanism of ϕ at the LHC. The phenomenological implications such as the DM relic density, DM direct and indirect detections have been extensively studied [4, 9–20].

If the DM particles can couple to the SM particles indirectly, the annihilation of the DM particles in the Galactic halo can generate extra flux of cosmic-ray particles and photons. Compared with the cosmic ray charged particles, the photons are not deflected by the Galactic magnetic fields and do not lose energy during the propagation in the Galactic halo. Thus they are of crucial importance in searching for the signals of halo DM annihilation.

The Galactic Center (GC) is expected to harbour high densities of DM, as suggested by N-body simulations, which makes it a promising place to look for photon signals of DM annihilation or decay. Recently, a number of groups including Fermi-LAT collaboration have independently found statistically strong evidence for an excess in cosmic gamma-ray fluxes at energy ~ 2 GeV towards the inner regions around the Galactic center (GC) from the data of Fermi-LAT [21–35]. The morphology of this GC excess (GCE) emission is consistent with a spherical emission profile expected from DM annihilation. The origin of the GCE is still under debate. There exists plausible astrophysical explanations such as the unresolved point sources of mili-second pulsars [24–27, 36, 37] and the interactions between the cosmic rays and the molecular gas [28, 29, 38]. Halo DM annihilation can also provide a reasonable explanation. The determined energy spectrum of the excess emission although depending on the choices of diffuse gamma-ray background templates, is in general compatible with the scenario of ~ 40 GeV DM particles self-annihilating into $b\bar{b}$ final states with a cross section $\langle\sigma v\rangle \approx (1 - 2) \times 10^{-26} \text{ cm}^3\text{s}^{-1}$ close to the typical thermal cross section for the observed DM relic abundance [30, 32] (other possible final states were considered in Refs. [19, 34, 39]).

The possible connection between the LHC diphoton excess and the GCE was first explored in [40]. Assuming a pseudoscalar ϕ which couples dominantly to gg , $\gamma\gamma$ and scalar DM particles, it was shown that the two reported photon excesses can be simultaneously explained if the total width of ϕ is large enough $\Gamma/M \gtrsim \mathcal{O}(10^{-2})$ which is favoured by the current ATLAS data. The phenomenological consequences of such a connection was further discussed in Refs. [41] and [42].

A large total width of ϕ , if confirmed, implies that the new physics sector is strongly coupled, or the resonance ϕ has large number of decay channels. In this work, we investigate the generic conditions for a consistent explanation for possible the LHC diphoton excess and GCE, especially the requirement on total width of ϕ in a wide range of DM models where the DM particle can be scalar, fermionic and vector, and ϕ can be generated by s -channel gluon fusion or quark-antiquark annihilation at parton level. We show that the minimally required ϕ width is determined by a single parameter proportional to $(m_\chi/M)^n$, where the integer n depends on the spins of the DM particle and its decay final states. We find that for scalar DM model with ϕ generated from $q\bar{q}$ annihilation, the minimally required Γ/M can be as low as $\mathcal{O}(10^{-3})$. For scalar DM model with ϕ generated from gg fusion and fermionic DM model with ϕ from $q\bar{q}$ annihilation, the required Γ/M reaches $\mathcal{O}(10^{-2})$. Other models such as the vector DM model requires larger Γ/M of order one which is already disfavoured by the current data. For the same DM model, the required width of ϕ is always smaller in $q\bar{q}$ channel than that in the gg channel. For the DM models which can simultaneously account for the diphoton excess and the GCE, the

predicted cross sections for gamma-ray line are typically of $\mathcal{O}(10^{-30}) \text{ cm}^3\text{s}^{-1}$, which is close to the current limits imposed by the Fermi-LAT data. These models can be distinguished by LHC and Fermi-LAT in the near future.

The rest of this paper is organized as follows. In section 2, we overview the interpretation of the diphoton excess, and derive model-independent conditions for a consistent explanation for the diphoton excess and the GCE. In section 3, we discuss model-independently the implications of the GCE for the DM properties. In section 4, we determine the allowed parameters in various DM models in which the DM particles can be scalar, fermionic and vector with ϕ generated by gg fusion and $q\bar{q}$ annihilation. The conclusion is given in section 5.

2 The LHC diphton excess

We consider the simplest scenario where the diphoton events are produced from the decay of the s -wave resonance ϕ which is generated through $X\bar{X}$ fusion or annihilation process, where $X\bar{X} = gg, \gamma\gamma$ and $q\bar{q}$ ($q = u, d, c, s, t, b$). The production cross section for the process $pp \rightarrow \phi \rightarrow \gamma\gamma$ in the narrow-width approximation is given by

$$\sigma_{\gamma\gamma} = \frac{2J+1}{(\Gamma/M)_s} \left(\sum_X C_{X\bar{X}} \frac{\Gamma_{X\bar{X}}}{M} \right) \left(\frac{\Gamma_{\gamma\gamma}}{M} \right), \quad (1)$$

where J is the spin of ϕ , and the coefficients $C_{X\bar{X}}$ incorporate the integration over the parton distribution functions of the protons. For instance, at the center-of-mass energy $\sqrt{s} = 13$ (8) TeV, $C_{gg} \approx 2137$ (174), $C_{b\bar{b}} \approx 15.3$ (1.07) and $C_{c\bar{c}} \approx 36$ (2.7) [4]. Higher order QCD corrections can be taken into account by including the K -factors with typical values $K_{gg} \text{ } (q\bar{q}) \approx 1.48$ (1.20). For the sake of simplicity, we consider the case where ϕ is spin zero, and one channel of $X\bar{X}$ dominates the ϕ production at a time. The process of $\gamma\gamma$ fusion is always included, as it is irreducible. In the limit of $\Gamma_{X\bar{X}} \gg \Gamma_{\gamma\gamma}$, the values of the partial decay widths required to account for the diphoton excess at Run-2 are estimated as

$$\left(\frac{\Gamma_{X\bar{X}}}{M} \right) \left(\frac{\Gamma_{\gamma\gamma}}{M} \right) \approx \frac{2.1 \times 10^{-4}}{C_{X\bar{X}}} \left(\frac{\sigma_{\gamma\gamma}}{8 \text{ fb}} \right) \left(\frac{\Gamma/M}{0.06} \right). \quad (2)$$

The non-observation of any excess at Run-1 (8 TeV) already imposes stringent limits on the cross sections for a number of final states generated from the decay of a generic resonance

$$\begin{aligned} \sigma_{Z\gamma} &\leq 4.0 \text{ fb} [43], \sigma_{ZZ} \leq 12 \text{ fb} [44], \sigma_{WW} \leq 40 \text{ fb} [45, 46], \\ \sigma_{\gamma\gamma} &\leq 1.5 \text{ fb} [47], \sigma_{jj} \leq 2.5 \text{ pb} [48], \sigma_{b\bar{b}} \leq 1.0 \text{ pb} [49], \end{aligned} \quad (3)$$

The enhancement of the production cross section at Run-2 relative to that at Run-1 can be described by the gain factor $r = \sigma_{13\text{TeV}}/\sigma_{8\text{TeV}} \approx 0.38 C_{X\bar{X}}(13\text{TeV})/C_{X\bar{X}}(8\text{TeV})$. In

order to account for an excess seen at Run-2 but not Run-1, a large value of r is favoured. The production channels with leading r factors are $r_{b\bar{b}} \approx 5.4$, $r_{gg} \approx 4.7$, and $r_{c\bar{c}} \approx 5.1$. Other channels have smaller gain factors, for instance, $r_{ss} \approx 4.3$, $r_{dd} \approx 2.7$, $r_{uu} \approx 2.5$, and $r_{\gamma\gamma} \approx 1.9$. Thus they are not considered further in this work. In the case where ϕ also couples to DM particles, the total width of ϕ is given by

$$\Gamma = \Gamma_{gg(q\bar{q})} + \kappa\Gamma_{\gamma\gamma} + \Gamma_{\chi\chi}, \quad (4)$$

where the factor $\kappa = (1 + \Gamma_{ZZ}/\Gamma_{\gamma\gamma} + \Gamma_{Z\gamma}/\Gamma_{\gamma\gamma} + \Gamma_{WW}/\Gamma_{\gamma\gamma})$ absorbs the contributions from ZZ , $Z\gamma$ and WW final states, which depends on the couplings between ϕ and the SM weak gauge bosons in a given model. If the total width Γ can be determined by the experiment, Eq. (4) can place an important constraint on the properties of the DM particle.

If the diphoton events are generated dominantly by the process of gluon fusion (quark-antiquark annihilation) $gg (q\bar{q}) \rightarrow \phi \rightarrow \gamma\gamma$, the cross sections of diphoton production and DM annihilation are strongly correlated, as the DM particles inevitably annihilate into these states through the same intermediate state, $\chi\bar{\chi} \rightarrow \phi \rightarrow gg, (q\bar{q}), \gamma\gamma$.

The same DM annihilation process determines both the DM relic density and the DM indirect detection signals. For the s -channel DM annihilation process $\chi\chi \rightarrow \phi \rightarrow X\bar{X}$, the corresponding thermally-averaged product of the DM annihilation cross section and the DM relative velocity can be written in a generic form

$$\langle\sigma v\rangle_{X\bar{X}} = \frac{8\pi\eta_\chi R_{X\bar{X}}}{s_\chi^2 \left[(1 - 4m_\chi^2/M^2)^2 + (\Gamma/M)^2 \right] m_\chi^2 \beta_\chi(M^2)} \left(\frac{\Gamma_{\chi\chi}}{M} \right) \left(\frac{\Gamma_{X\bar{X}}}{M} \right), \quad (5)$$

where $\eta_\chi = 2$ (1) for the DM particle (not) being its own antiparticle, s_χ is the spin degrees-of-freedom of the DM particle with $s_\chi = 1, 2$ and 3 for the DM being a scalar, fermion and vector, respectively. The quantity $\beta_X(s) \equiv (1 - 4m_X^2/s)^{1/2}$ is the velocity of the particle X from the decay $\phi^{(*)} \rightarrow X\bar{X}$ with a squared center-of-mass energy s . The function $R_{X\bar{X}}$ is essentially the ratio of ϕ decay squared amplitudes at $s \approx 4m_\chi^2$ and M^2

$$R_{X\bar{X}}(m_\chi^2/M^2) = \frac{\sum |M_{\phi \rightarrow \chi\chi}(s = 4m_\chi^2)|^2 \sum |M_{\phi \rightarrow X\bar{X}}(s = 4m_\chi^2)|^2 \beta_X(4m_\chi^2)}{\sum |M_{\phi \rightarrow \chi\chi}(s = M^2)|^2 \sum |M_{\phi \rightarrow X\bar{X}}(s = M^2)|^2 \beta_X(M^2)}. \quad (6)$$

For a consistent explanation of the diphoton excess and the GCE, Eqs. (1), (4) and (5) must be satisfied simultaneously. The corresponding solutions for the ϕ partial decay widths in the limits $m_\chi/M \ll 1$ and $\Gamma/M \ll 1$ are given by

$$\left(\frac{\Gamma_{X\bar{X}}}{M} \right) = \frac{1}{2} \left[\left(\frac{\Gamma}{M} \right) \pm \Delta^{1/2} \right], \quad \left(\frac{\Gamma_{\gamma\gamma}}{M} \right) = \frac{\sigma_{\gamma\gamma} s (\Gamma/M)}{C_{X\bar{X}} (\Gamma_{X\bar{X}}/M)}, \quad (7)$$

where

$$\Delta \equiv \left(\frac{\Gamma}{M} \right)^2 - 4 \left[\frac{s_\chi^2 m_\chi^2 \beta_\chi(M^2) \langle\sigma v\rangle_{X\bar{X}}}{8\pi\eta_\chi R_{X\bar{X}}} + \frac{\kappa\sigma_{\gamma\gamma} s}{C_{X\bar{X}}} \frac{\Gamma}{M} \right]. \quad (8)$$

The necessary condition for the existence of the solutions is $\Delta \geq 0$. As it can be seen in the following sections, in most DM models $R_{X\bar{X}} \propto (m_\chi/M)^{2n}$, ($n = 1, 2, 3, \dots$). Since we are interested in the case of GCE where $m_\chi \ll M$, the second term in the square brackets in Eq. (8) can be safely neglected. In a good approximation, the condition can be written as

$$\frac{\Gamma}{M} \gtrsim \left(\frac{s_\chi^2 m_\chi^2 \beta_\chi \langle \sigma v \rangle_{X\bar{X}}}{2\pi \eta_\chi R_{X\bar{X}}} \right)^{1/2}. \quad (9)$$

For a given DM model, the factor $R_{X\bar{X}}$ is fixed. If the diphoton excess is consistent with the DM thermal relic density which is set by DM annihilation into $X\bar{X}$, then the annihilation cross section must be close to the typical thermal cross section $\langle \sigma v \rangle_{X\bar{X}} \approx \langle \sigma v \rangle_F = 3 \times 10^{-26} \text{ cm}^3\text{s}^{-1}$. From the value of Γ/M determined by the experiment, one can derive an upper limit on $\langle \sigma v \rangle_{X\bar{X}}$ as a function of m_χ from Eq. (9), which depends on the nature of the DM particle and the final state $X\bar{X}$. On the other hand, if the diphoton excess is required to be consistent with the GCE, since both $\langle \sigma v \rangle_{X\bar{X}}$ and m_χ can be determined by the GCE data, Eq. (9) can lead to a minimal requirement on the total width Γ/M .

The diphoton excess suggests that the DM particles inevitably annihilate into two-photon final states through s -channel ϕ exchange, which results in a spectral line in the generated gamma-ray flux with photon energy centered at $E_\gamma = m_\chi$. The spectral line is difficult to be mimicked by conventional astrophysical contributions, if observed, can be a strong evidence for halo DM annihilation or decay. If the diphoton excess is generated from $X\bar{X}$ initial states, from Eq. (1) and (5), it follows that

$$\langle \sigma v \rangle_{\gamma\gamma} = \frac{\sigma_{\gamma\gamma}}{\sigma_{X\bar{X}}} \frac{R_{\gamma\gamma}}{R_{X\bar{X}}} \langle \sigma v \rangle_{X\bar{X}}, \quad (10)$$

where $\sigma_{X\bar{X}}$ is the cross section for the production of $X\bar{X}$ final states through intermediate state ϕ from $X\bar{X}$ fusion or annihilation at the LHC, i.e. $X\bar{X} \rightarrow \phi \rightarrow X\bar{X}$. For a given DM model, the values of $R_{\gamma\gamma}/R_{X\bar{X}}$ is fixed. Thus, from the Run-1 upper limit on $\sigma_{X\bar{X}}$, one can obtain a *lower* limit on $\langle \sigma v \rangle_{\gamma\gamma}$. It was shown in Ref. [40] that a lower limit of $\langle \sigma v \rangle_{\gamma\gamma} \gtrsim 4.8 \times 10^{-30} \text{ cm}^3\text{s}^{-1}$ can be obtained in a scalar DM model with ϕ generated through gg fusion.

If ϕ is allowed to couple to $Z\gamma$, the DM annihilation can generate a gamma-ray line with photon energy at $E_\gamma = m_\chi(1 - m_Z^2/4m_\chi^2)$. The annihilation cross section for the process $\chi\chi \rightarrow \phi \rightarrow Z\gamma$ is related to that for $\chi\chi \rightarrow \phi \rightarrow \gamma\gamma$ as follows

$$\langle \sigma v \rangle_{Z\gamma} = \frac{\sigma_{Z\gamma}}{\sigma_{\gamma\gamma}} \frac{\tilde{\beta}_Z^6(4m_\chi^2)}{\tilde{\beta}_Z^6(M^2)} \langle \sigma v \rangle_{\gamma\gamma}, \quad (11)$$

where $\tilde{\beta}_X(s) = (1 - m_X^2/s)^{1/2}$. Since $\sigma_{Z\gamma}/\sigma_{\gamma\gamma}$ is a known in a give model, a lower limit on $\langle \sigma v \rangle_{Z\gamma}$ can be obtained in a similar way.

3 The Galactic Center Excess

The annihilation of DM particles into $X\bar{X}$ final states generates diffuse gamma rays with a broad energy spectrum due to hadronization, while the annihilation into $\gamma\gamma$ generates a line-shape spectrum with energy centered at the DM particle mass. Both the signatures are under active searches by the current DM indirect detection experiments. The differential gamma-ray flux, averaged over a solid angle $\Delta\Omega$ is given by

$$\frac{d\Phi}{dE} = \frac{\eta_X \rho_0^2 r_\odot}{16\pi} \frac{\langle\sigma v\rangle}{m_\chi^2} \frac{dN_\gamma}{dE} J, \quad (12)$$

where $r_\odot \approx 8.5$ kpc is the distance from the Sun to the GC, $\rho_0 \approx 0.4$ GeV/cm³ is the local DM density in the solar neighbourhood, and dN_γ/dE is the gamma-ray spectrum per DM annihilation. The dimensionless J -factor which contains the information of DM density distribution is given by

$$J = \int \frac{d\Omega}{\Delta\Omega} \int_{\text{l.o.s}} \left(\frac{\rho(r)}{\rho_0} \right)^2 \frac{ds}{r_\odot}, \quad (13)$$

where $\rho(r)$ is the spatial distribution of halo DM energy density, with r the distance to the GC. The integration is to be performed over the distance s along the light-of-sight which is related to r through the relation $r^2 = r_\odot^2 + s^2 - 2sr_\odot \cos\psi$, where ψ is the angle of the direction away from the GC. N-body simulations suggest an universal DM density profile of the Navarro-Frenk-White (NFW) form [50]

$$\rho(r) = \rho_s \left(\frac{r}{r_s} \right)^{-\gamma} \left[1 + \left(\frac{r}{r_s} \right)^\alpha \right]^{\frac{\gamma-\beta}{\alpha}}, \quad (14)$$

which is characterized by the parameters α , β , γ , and a reference scale $r_s \simeq 20$ kpc. For the standard NFW profile, $\alpha = \gamma = 1$ and $\beta = 3$. The normalization factor ρ_s is determined by the local DM density $\rho(r_\odot) = \rho_0$.

We determine the favoured values of m_χ and $\langle\sigma v\rangle_{X\bar{X}}$ for a number of annihilation final states such as gg , $b\bar{b}$, $c\bar{c}$ and $u\bar{u}$, from fitting to the GCE data derived in Ref. [34]. In total there are 24 data points. The spectra of the prompt gamma rays dN_γ/dE for DM annihilating into $X\bar{X}$ are generated by the Monte-Carlo simulation package Pythia 8.201 [51]. For the considered final states, the contributions from the inverse Compton scatterings can be safely neglected. We choose a modified NFW profile with an inner slope $\gamma = 1.26$, as suggested by the observed morphology of the gamma-ray emission [26, 27, 30, 34]. Making use of Eq. (12), the calculated diffuse gamma-ray fluxes are averaged over a square region of interest (ROI) $20^\circ \times 20^\circ$ in the sky with latitude $|b| < 2^\circ$ masked out. The corresponding J -factor is $J = 57.6$. The best-fit DM particle masses and annihilation cross sections, and the corresponding χ^2 and p -values are summarized in Tab. 1. In Fig. 1,

Channel	m_χ (GeV)	$\langle\sigma v\rangle_{bb}$ ($10^{-26}\text{cm}^3\text{s}^{-1}$)	$\chi^2_{\text{min}}/\text{d.o.f.}$	p -value
$b\bar{b}$	$46.15^{+5.81}_{-3.53}$	$1.42^{+0.18}_{-0.17}$	24.572/22	0.32
$c\bar{c}$	$35.54^{+3.10}_{-4.12}$	$0.95^{+0.12}_{-0.12}$	25.626/22	0.27
$u\bar{u}$	$22.26^{+2.83}_{-1.91}$	$0.62^{+0.10}_{-0.08}$	28.495/22	0.16
gg	$62.01^{+6.56}_{-6.35}$	$1.96^{+0.26}_{-0.24}$	24.665/22	0.31

TAB. 1: Values of DM mass and annihilation cross sections determined from fitting to the GCE data. The DM particle is assumed to be its own antiparticle.

we show the contours of the allowed regions for the parameters m_χ and $\langle\sigma v\rangle_{X\bar{X}}$ at 68% and 95% C.L. for two parameters, corresponding to $\Delta\chi^2 = 2.3$ and 6.0, respectively. As can be seen from the table, in the DM interpretation of the GCE, the required DM particle mass is in the range $\sim (20 - 70)$ GeV with a cross section $(0.5 - 2) \times 10^{-26}\text{cm}^3\text{s}^{-1}$. The most favoured channel is $b\bar{b}$. We emphasize that the gg channel also gives reasonably good fit with a larger DM mass ~ 60 GeV, which is crucial for a consistent explanation with the diphoton excess, as gg fusion is also the favoured channel for the production of ϕ at the LHC Run-2. These results are in good agreement with the previous analysis in Ref. [52].

At present, the most stringent constraints on the DM annihilation cross sections are provide by the Fermi-LAT data on the diffuse gamma rays of the dwarf spheroidal satellite galaxies (dSphs) [53]. These limits are also shown in Fig. 1 for comparison purpose, where the limits on gg channel was derived using a conservative rescaling approach detailed in Ref. [40]. It is known that there is an apparent tension between the GCE favoured regions and the Fermi-LAT limits. Note that the DM velocity dispersion in the Galactic halo is quite different from that in the dSphs. The DM annihilation cross section favoured by the GCE data and constrained by the gamma rays of dSphs can only be compared under the assumption that the cross section is velocity independent, which is in general not the case. In the analysis of the Fermi-LAT collaboration, the uncertainties in the J -factors were taken into account assuming a NFW type parametrization of the DM density profile. A recent analysis directly using the spherical Jeans equations rather than taking a parametric DM density profile as input showed that the J -factor can be smaller by a factor about 2 – 4 for the case of Ursa Minor, which relaxes the constraints on the DM annihilation cross section to the same amount [54].

The annihilation of halo DM also generates cosmic-rayparticles such as protons/antiprotons, electrons/positrons and neutrinos. Compared with gamma-rays, the predictions for the flux of cosmic-ray charged particles from DM annihilation suffer from large uncertainties in the cosmic-ray propagation models. For a DM particle mass below ~ 100 GeV, the predicted \bar{p}/p ratio peaks at lower energies below ~ 10 GeV, which suffer from additional

uncertainties due to the solar activities. The upper limits on the DM annihilation cross section from the AMS-02 and PAMELA data on \bar{p}/p ratio for various channels have been studied for various propagation models and DM density profiles (see e.g. [55–60]). In general, the obtained limits are weaker than that derived from the gamma rays of dSphs. The constraints from the cosmic-ray positrons depends strongly on the annihilation final states. For leptonic final states such as e^+e^- and $\mu^+\mu^-$, the derived upper limits from the AMS-02 positron flux can reach the typical thermal cross section for DM particle mass below 50–100 GeV [61]. But for hadronic final states such as $b\bar{b}$, the corresponding limits are rather weak, typically at $\mathcal{O}(10^{-24}) \text{ cm}^3\text{s}^{-1}$. The gg final state generates a softer positron spectrum in comparison with the $b\bar{b}$ final states. Thus the corresponding limits are expected to be even weaker.

4 DM Models

We focus on the scenario where the 750 GeV resonance ϕ is a pseudo-scalar particle. For a scalar resonance, the related couplings are severely constrained by the null results of the DM direct detection experiments. The UV origins of the pseudoscalar ϕ can be axion-like particles from the breaking of the Peccei-Quinn symmetry [62], pseudo-Goldstone boson from composite Higgs models [63], or from the extended Higgs sectors of the SM [64–72], or left-right symmetric models [73–82]. If ϕ is a SM singlet and couples to the SM gauge bosons through vector-like heavy fermions which have small mixings with the SM fermions, the constraints from the oblique parameters S and T , the EW precision test, and the flavor physics can be relaxed [83]. A pseudo-scalar does not mix with the SM Higgs boson, and is less constrained by the measured properties of the Higgs boson. For fermionic DM, its annihilation into SM particles through s -channel pseudoscalar exchange is not suppressed by the low velocity dispersion of the halo DM. Since ϕ is a pseudo-scalar, the cross sections for DM-nucleus scattering through quarks or gluons within the nucleus are either velocity suppressed or vanishing, which easily relaxes the stringent upper limits from various DM direct detection experiments.

We assume that ϕ can couple to the SM quarks directly and the SM gauge fields indirectly through loop processes (see e.g. Refs. [84]). Since ϕ is much heavier than the electroweak (EW) scale, we start with EW gauge-invariant effective interactions up to dimension-five

$$\begin{aligned} \mathcal{L} \supset & \frac{1}{2} \partial_\mu \phi \partial^\mu \phi - \frac{1}{2} M^2 \phi^2 - i y_q \bar{q} \gamma^5 q \phi - \frac{g_1^2}{2\Lambda} \phi B_{\mu\nu} \tilde{B}^{\mu\nu} \\ & - \frac{g_2^2}{2\Lambda} \phi W_{\mu\nu} \tilde{W}^{\mu\nu} - \frac{g_g^2}{2\Lambda} \phi G_{\mu\nu} \tilde{G}^{\mu\nu}, \end{aligned} \quad (15)$$

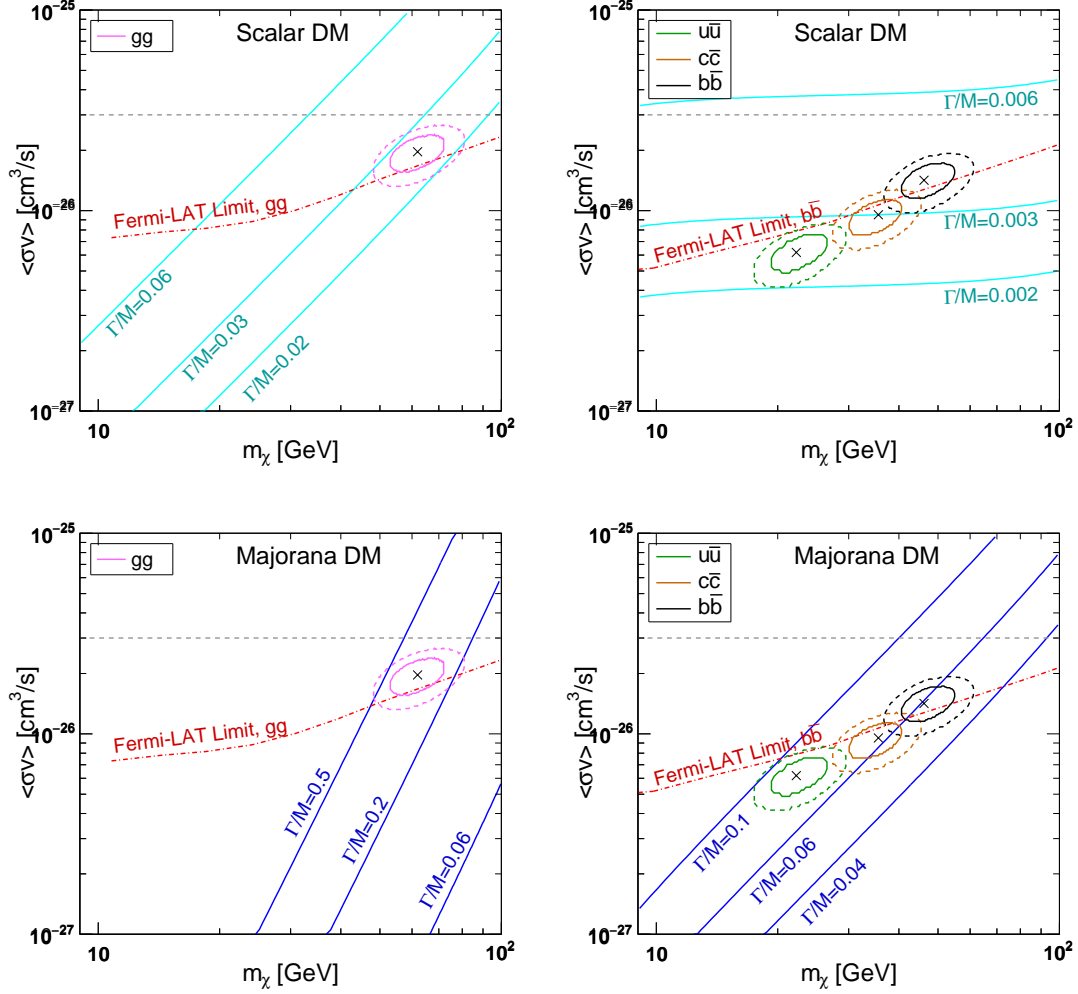


FIG. 1: Upper panels) Left: regions of DM mass and annihilation cross section allowed by the GCE data at 68% and 95% C.Ls. for the scalar DM particle annihilating into gg final states through ϕ exchange. Upper limits on the annihilation cross section as a function of DM particle mass for fixed values of Γ/M are shown. See text for detailed explanations. The horizontal line indicates the typical thermal annihilation cross section of $3 \times 10^{-26} \text{ cm}^3\text{s}^{-1}$. The 95% C.L. upper limits from the Fermi-LAT data on the gamma rays from dSphs [53] are also shown. The limits on gg channel was derived using a conservative rescaling approach detailed in [40]. Right: the same as left but for DM annihilation into $b\bar{b}$, $c\bar{c}$ and $u\bar{u}$ final states. Lower pannels) The same as upper panels but for Majorana fermionic DM model.

where for the gauge fields $\tilde{F}_{\mu\nu} = \frac{1}{2}\epsilon_{\mu\nu\alpha\beta}F^{\alpha\beta}$, $g_{1,2,g}$ are the dimensionless effective coupling strengths, y_q is the Yukawa coupling strength, and Λ is a common energy scale. After the EW symmetry breaking, the interaction terms involving physical EW gauge bosons A , Z and W are given by

$$\begin{aligned}\mathcal{L}_{\text{gauge}} \supset & -\frac{g_A^2}{2\Lambda}\phi A_{\mu\nu}\tilde{A}^{\mu\nu} - \frac{g_Z^2}{2\Lambda}\phi Z_{\mu\nu}\tilde{Z}^{\mu\nu} - \frac{g_{AZ}^2}{2\Lambda}\phi A_{\mu\nu}\tilde{Z}^{\mu\nu} \\ & - \frac{g_W^2}{2\Lambda}\phi W_{\mu\nu}\tilde{W}^{\mu\nu} - \frac{g_g^2}{2\Lambda}\phi G_{\mu\nu}\tilde{G}^{\mu\nu},\end{aligned}\quad (16)$$

where the physical gauge couplings g_A , g_Z , g_{ZA} and g_W are related to that in the gauge basis as

$$\begin{aligned}g_A^2 &= g_1^2 c_W^2 + g_2^2 s_W^2, & g_Z^2 &= g_1^2 s_W^2 + g_2^2 c_W^2, \\ g_{ZA}^2 &= 2s_W c_W (g_2^2 - g_1^2), & g_W^2 &= g_2^2\end{aligned}\quad (17)$$

with $s_W^2 = 1 - c_W^2 = \sin^2 \theta_W \approx 0.23$. For the three extreme cases: $g_1 = 0$, $g_1 = g_2$ and $g_2 = 0$, the partial widths of ZZ , $Z\gamma$ and WW relative to that of $\gamma\gamma$ and the values of κ are listed in Tab. 2. We should focus on the case of $g_2 = 0$, namely ϕ is not charged under the $SU(2)_L$ gauge group. Note that the case of $g_1 = 0$ is severely constrained by the Run-I data on the $Z\gamma$ and ZZ production rates, as it can be seen from Eq. (3) and Tab. 2. The related phenomenology in the case of $g_1 = g_2$ is similar to that in the case of $g_2 = 0$, except that the DM annihilation into $Z\gamma$ is forbidden. Thus there is no gamma-ray line generated from $Z\gamma$ final states.

The partial decay widths for ϕ decaying into the SM gauge bosons and the fermions are given by

$$\frac{\Gamma_{\gamma\gamma}}{M} = \pi\alpha_A^2 \left(\frac{M}{\Lambda}\right)^2, \quad \frac{\Gamma_{gg}}{M} = 8\pi\alpha_g^2 \left(\frac{M}{\Lambda}\right)^2, \quad \frac{\Gamma_{q\bar{q}}}{M} = \frac{3y_q^2\beta_q(M^2)}{8\pi}, \quad (18)$$

respectively, where $\alpha_{A,g} = g_{A,g}^2/4\pi$. For the spin nature of DM particles, we consider three classes of models where the DM particles can be scalar, fermionic and vector.

4.1 Real scalar DM

In the real scalar DM model, the Lagrangian for the DM particle χ and its interaction with ϕ is given by

$$\mathcal{L} \supset \frac{1}{2}\partial_\mu\chi\partial^\mu\chi - \frac{1}{2}m_\chi^2\chi^2 - \frac{1}{2}g_\chi\phi\chi^2, \quad (19)$$

where g_χ is a dimensionful coupling strength, and we have only included the most relevant interaction term. Other possible interaction terms such as $\lambda\phi^2\chi^2/4$ are neglected by assuming small couplings.

models	$\Gamma_{ZZ}/\Gamma_{\gamma\gamma}$	$\Gamma_{Z\gamma}/\Gamma_{\gamma\gamma}$	$\Gamma_{WW}/\Gamma_{\gamma\gamma}$	κ
$g_1 = 0$	10	6.4	35	53
$g_1 = g_2$	0.9	0	1.9	3.8
$g_2 = 0$	0.081	0.57	0	1.7

TAB. 2: Ratios of ϕ decay widths $\Gamma_{ZZ}/\Gamma_{\gamma\gamma}$, $\Gamma_{Z\gamma}/\Gamma_{\gamma\gamma}$, $\Gamma_{WW}/\Gamma_{\gamma\gamma}$ and the value of κ defined in Eq. (4) for three cases of ϕ couplings with the SM gauge bosons, $g_1 = 0$, $g_1 = g_2$ and $g_2 = 0$, respectively.

For DM annihilation into gg final states, the corresponding factor R_{gg} defined in Eq. (5) is given by

$$R_{gg} = 16 \left(\frac{m_\chi}{M} \right)^4, \quad (20)$$

which is typically of $\mathcal{O}(10)^{-4}$ for $m_\chi \approx 60$ GeV. In this case, Eq. (9) can be rewritten as

$$\left(\frac{\Gamma}{M} \right)_{\text{scalar}, gg} \geq \frac{\beta_\chi^{1/2} (M^2) \langle \sigma v \rangle_{gg}^{1/2} M^2}{8\pi^{1/2} m_\chi}. \quad (21)$$

For a given value of Γ/M , the above inequality can be interpreted as the upper limit on $\langle \sigma v \rangle_{gg}$ as a function of m_χ . In the upper-left panel of Fig. 1, we show this relation for three choices of $\Gamma/M = 0.06$, 0.03 and 0.02 , respectively. If $\langle \sigma v \rangle_{gg}$ is required to meet the thermal value $\langle \sigma v \rangle_F$, it can be seen that the DM particle mass has to be larger than ~ 65 GeV (90 GeV) for $\Gamma/M = 0.03$ (0.02). While for $\Gamma/M = 0.06$, the constraint on the DM particle mass is rather weak.

If Γ/M is not fixed, using the best-fit values of m_χ and $\langle \sigma v \rangle_{gg}$ for gg channel from Tab. 1, a lower limit on the required total width of ϕ can be obtained as follows

$$\left(\frac{\Gamma}{M} \right)_{\text{scalar}, gg} \gtrsim 0.026 \left(\frac{M}{750 \text{ GeV}} \right)^2 \left(\frac{62 \text{ GeV}}{m_\chi} \right) \left(\frac{\langle \sigma v \rangle_{gg}}{2.0 \times 10^{-26} \text{ cm}^3 \text{s}^{-1}} \right)^{1/2}. \quad (22)$$

Thus the GCE required typical minimal width-to-mass ratio is quite large of $\mathcal{O}(10^{-2})$, which is currently favoured by ATLAS, and can be confirmed or ruled out soon by the upcoming LHC updated results. Assuming ϕ is generated dominantly by gg fusion, a combined fit to both the data of diphton excess and GCE in this model has been carried out in Ref. [40], which showed that the total width of ϕ is dominated by $\Gamma_{\chi\chi}$, and the favoured partial widths Γ_{gg}/M and $\Gamma_{\gamma\gamma}/M$ are of $\mathcal{O}(10^{-3})$ and $\mathcal{O}(10^{-5})$, respectively.

According to Eq. (7), there are actually two solutions for Γ_{gg}/M . We update the previous analysis by considering wider ranges of parameters and including the contribution from photon fusion which is non-negligible when Γ_{gg}/M is below $\mathcal{O}(10^{-4})$. In Fig. 2, we

show the regions of the partial decay widths allowed by the diphoton excess and GCE in wide ranges of parameter space in $(\Gamma_{gg}/M, \Gamma_{\gamma\gamma}/M)$ and $(\Gamma_{\chi\chi}/M, \Gamma_{\gamma\gamma}/M)$ planes. The allowed regions are at 68% and 95% C.Ls. for two parameters, corresponding to $\Delta\chi^2 = 2.3$ and 6.0, respectively, together with the allowed regions by each individual experiment, for the case of $\Gamma/M = 0.06$ and 0.03. It can be clearly seen that there is another solution located at $\Gamma_{gg}/M \approx \Gamma/M$ which corresponds to the case where the total width is dominated by gluon final states. However, this solution is ruled out by the limit on the dijet production at Run-1, as can be seen from the figure.

If the diphoton events are generated from parton level $q\bar{q}$ annihilation, the situation is quite different. For $q\bar{q}$ annihilation channel, the function $R_{q\bar{q}}$ is given by

$$R_{q\bar{q}} = 4 \frac{\beta_q(4m_\chi^2)}{\beta_q(M^2)} \left(\frac{m_\chi}{M} \right)^2, \quad (23)$$

Since $R_{q\bar{q}}$ is proportional to $(m_\chi/M)^2$ instead of $(m_\chi/M)^4$, the lower limit on Γ/M can be much smaller. For DM annihilation dominantly into $b\bar{b}$ final states, Eq. (9) can be rewritten as

$$\left(\frac{\Gamma}{M} \right)_{\text{scalar}, b\bar{b}} \gtrsim \frac{\beta_\chi^{1/2}(M^2) \langle \sigma v \rangle_{b\bar{b}}^{1/2} M}{4\pi^{1/2}}. \quad (24)$$

Note that for $b\bar{b}$ final states, it is determined by $\langle \sigma v \rangle_{b\bar{b}}$ alone, as the leading m_χ dependence cancels out in Eq. (9). This observation holds for all the $q\bar{q}$ final states. In the upper-right panel of Fig. 1, we show the maximally allowed value of $\langle \sigma v \rangle$ as a function of DM particle mass for three choices of $\Gamma/M = 0.006, 0.003$ and 0.002, respectively. If $\langle \sigma v \rangle_{b\bar{b}}$ is required to be equal to $\langle \sigma v \rangle_F$, we find that the required Γ/M should be above ~ 0.006 , which is insensitive to the DM particle mass.

Using the best-fit values of m_χ and $\langle \sigma v \rangle_{b\bar{b}}$ for $b\bar{b}$ channel in Tab. 1, the corresponding minimal value of the width-to-mass ratio is found to be

$$\left(\frac{\Gamma}{M} \right)_{\text{scalar}, b\bar{b}} \gtrsim 3.6 \times 10^{-3} \left(\frac{M}{750 \text{ GeV}} \right) \left(\frac{\langle \sigma v \rangle_{b\bar{b}}}{1.4 \times 10^{-26} \text{ cm}^3 \text{s}^{-1}} \right)^{1/2}. \quad (25)$$

Similarly, for the $c\bar{c}$ channel, the minimal width is given by

$$\left(\frac{\Gamma}{M} \right)_{\text{scalar}, c\bar{c}} \gtrsim 3.0 \times 10^{-3} \left(\frac{M}{750 \text{ GeV}} \right) \left(\frac{\langle \sigma v \rangle_{c\bar{c}}}{0.95 \times 10^{-26} \text{ cm}^3 \text{s}^{-1}} \right)^{1/2}. \quad (26)$$

Thus for $q\bar{q}$ annihilation, the required minimal width-to-mass ratio can be reduced to $\mathcal{O}(10^{-3})$, an order of magnitude lower than that in the case of gg fusion.

We perform analogous χ^2 fits to the data of diphoton excess and the GCE in $b\bar{b}$ and $c\bar{c}$ channels to determine the allowed values of the parameters m_χ , $\Gamma_{\chi\chi}/M$, $\Gamma_{q\bar{q}}/M$

and $\Gamma_{\gamma\gamma}/M$ for two typical values of total width $\Gamma/M = 0.06$ and 0.006 , respectively. For the diphoton excess, we take a naively weighted average of ATLAS and CMS results $\sigma_{\gamma\gamma} = 8 \pm 2.1$ fb. The Run-1 limits on dijet and diphoton productions are taken into account. For the fit to the GCE, the data and the selection of the region of interest in the sky are the same as the fit in Sec. 3. The results of the best-fit values and uncertainties of these parameters are summarized in Tab. 3. Compared with the fits to the GCE data alone, there are no significant changes in the determined DM particle mass. The values of $\chi^2/\text{d.o.f}$ are also comparable, which indicates that the diphoton excess and GCE can be consistently explained in this model.

The allowed regions for the partial decay widths at 68% and 95% C.Ls., together with the allowed regions by each individual experiment, for the case of $\Gamma/M = 0.06$ (0.006) are shown in Fig. 3 (Fig. 4). For the $q\bar{q}$ annihilation channels, the two solutions of Eq. (7) can be seen as the two well-separated regions characterized by

$$\begin{aligned} \frac{\Gamma_{\chi\chi}}{M} &\approx \frac{\Gamma}{M}, & \frac{\Gamma_{q\bar{q}}}{M} &\ll \frac{\Gamma_{\chi\chi}}{M}, & \text{(i)} \\ \frac{\Gamma_{q\bar{q}}}{M} &\approx \frac{\Gamma}{M}, & \frac{\Gamma_{\chi\chi}}{M} &\ll \frac{\Gamma_{q\bar{q}}}{M}. & \text{(ii)} \end{aligned} \quad (27)$$

The solution (i) corresponds to case of DM dominance while the solution (ii) corresponds to the quark dominance in the total width. In $q\bar{q}$ channels, the Run-1 dijet constraint does not apply. However, the Run-1 constraint on the diphoton production cross section $\sigma_{\gamma\gamma}$ becomes relevant. In the large width case with $\Gamma/M = 0.06$, for both the $b\bar{b}$ and $c\bar{c}$ channels, the solution (i) is ruled out by the Run-1 limit on the diphoton production, as the required $\Gamma_{\gamma\gamma}$ is above $\mathcal{O}(10^{-3})$. The solution (ii) is consistent with the data, and the favoured $\Gamma_{\chi\chi}/M$ are of $\mathcal{O}(10^{-5})$, and $\Gamma_{\gamma\gamma}/M$ are of $\mathcal{O}(10^{-4})$. In the solution (ii), from $\Gamma_{q\bar{q}}/M \approx \Gamma/M = 0.06$, the size of the Yukawa coupling is found to be $y_q^2 \approx 0.5$ which is marginally within the perturbative regime. In the small width case with $\Gamma/M = 0.006$, for $b\bar{b}$ channel, both the solutions are close to the Run-1 diphoton limit. But the solution (ii) is favoured against solution (i). For the $c\bar{c}$ channel, the situation is similar. In the small width case $\Gamma/M = 0.006$, the favoured $\Gamma_{\chi\chi}/M$ is comparable with $\Gamma_{\gamma\gamma}$, both are of $\mathcal{O}(10^{-4})$. The determined values of m_χ and $\langle\sigma v\rangle_{b\bar{b},c\bar{c}}$ for the solution (ii) are listed in Tab. 3.

Since in the $q\bar{q}$ channel, the total width is not DM dominated. The predicted cross section for gamma-ray lines which is proportional to $\Gamma_{\chi\chi}\Gamma_{\gamma\gamma}$ can be smaller. In Fig. 6, we give the predicted cross sections for DM annihilation into $\gamma\gamma$ which gives rise to the gamma-ray spectral lines, based on the parameters determined from the fit results listed in Tab. 3 for $b\bar{b}$ and $c\bar{c}$ channels with two different values of $\Gamma/M = 0.06$ and 0.006 , respectively. In all the cases the predictions are well below the current upper limits set by Fermi-LAT. For $\Gamma/M = 0.06$, the predicted cross section $\langle\sigma v\rangle_{\gamma\gamma}$ is $\sim 5 \times 10^{-31} \text{ cm}^3\text{s}^{-1}$

Channel	Γ/M	m_χ (GeV)	$\Gamma_{\gamma\gamma}/M(\times 10^{-4})$	$\Gamma_{\chi\chi}/M$	$\chi^2_{\min}/\text{d.o.f.}$	p -value
Scalar DM, $b\bar{b}$	0.06	$46.15^{+5.81}_{-3.53}$	$1.90^{+0.49}_{-0.50}$	$5.52^{+0.68}_{-0.68} \times 10^{-5}$	25.418/23	0.33
	0.006	$46.15^{+5.81}_{-3.53}$	$2.04^{+0.46}_{-0.48}$	$6.56^{+0.97}_{-0.92} \times 10^{-4}$	24.578/23	0.37
Scalar DM, $c\bar{c}$	0.06	$35.54^{+3.10}_{-4.12}$	$0.81^{+0.21}_{-0.21}$	$3.80^{+0.47}_{-0.47} \times 10^{-5}$	26.664/23	0.27
	0.006	$35.54^{+3.10}_{-4.12}$	$0.89^{+0.23}_{-0.23}$	$4.11^{+0.56}_{-0.54} \times 10^{-4}$	26.311/23	0.29
Fermionic DM, $b\bar{b}$	0.06	$46.20^{+6.37}_{-2.68}$	$4.55^{+2.39}_{-2.11}$	$3.49^{+0.85}_{-1.75} \times 10^{-2}$	24.906/23	0.36
Fermionic DM, $c\bar{c}$	0.06	$36.48^{+3.13}_{-2.11}$	$1.62^{+0.82}_{-0.55}$	$3.01^{+0.81}_{-0.85} \times 10^{-2}$	27.048/23	0.25

TAB. 3: Values of DM mass m_χ , partial width-to-mass ratios $\Gamma_{\gamma\gamma}/M$ and $\Gamma_{\chi\chi}/M$ determined from combined fits to both the LHC diphoton excess and the GCE in scalar and fermionic DM models with constraints from Run-1 data on the dijet and diphoton searches included. For scalar DM models, the results for the cases of ϕ coupling dominantly to $b\bar{b}$ or $c\bar{c}$ with total width $\Gamma/M = 0.06$ and 0.006 are given. For fermionic DM models, the results are for $\Gamma/M = 0.06$. The corresponding $\chi^2/\text{d.o.f}$ and p -values for each fit are also shown.

for $b\bar{b}$ channel, and $\langle\sigma v\rangle_{Z\gamma}$ is below $\sim 10^{-31} \text{ cm}^3\text{s}^{-1}$. For $c\bar{c}$ channel, the predicted cross section $\langle\sigma v\rangle_{\gamma\gamma}$ is $\sim 1 \times 10^{-31} \text{ cm}^3\text{s}^{-1}$. The $Z\gamma$ final state is kinematically forbidden due to the low mass of the DM particle. For $\Gamma/M = 0.06$, the predictions are relatively higher, which is due to the fact that a larger $\Gamma_{\chi\chi}/M$ of $\mathcal{O}(10^{-4})$ is favoured.

4.2 Fermionic DM

For fermionic DM, we shall focus on the case where χ is a Majorana fermion. The results for the Dirac DM particle can be obtained in a straight forward way. The Lagrangian for the Majorana DM particle and its interaction with ϕ is given by

$$\mathcal{L} \supset \frac{1}{2}\bar{\chi}(i\gamma^\mu\partial_\mu - m_\chi)\chi - \frac{1}{2}y_\chi\bar{\chi}i\gamma^5\chi\phi. \quad (28)$$

For the DM annihilation into gg and $q\bar{q}$ final states, the corresponding $R_{X\bar{X}}$ factors are

$$R_{gg} = 64 \left(\frac{m_\chi}{M}\right)^6 \quad \text{and} \quad R_{q\bar{q}} = 16 \frac{\beta_q(4m_\chi^2)}{\beta_q(M^2)} \left(\frac{m_\chi}{M}\right)^4. \quad (29)$$

For gg annihilation final states in this model, the Eq. (9) can be written as

$$\left(\frac{\Gamma}{M}\right)_{\text{fermion}, gg} \geq \frac{\beta_\chi^{1/2}(M^2)\langle\sigma v\rangle_{gg}^{1/2} M^3}{8\pi^{1/2}m_\chi^2}. \quad (30)$$

Since in this model the R_{gg} factor is proportional to $(m_\chi/M)^6$, the required total width is quite large. In the lower-left panel of Fig. 1, we show the upper limit on $\langle\sigma v\rangle_{gg}$ as a

function of m_χ for three choices of $\Gamma/M = 0.5, 0.2$ and 0.06 , respectively. For DM particle mass below ~ 100 GeV, the value of $\langle\sigma v\rangle_{gg}$ is far below the typical thermal cross section. For a consistent explanation to the DM relic density, the required DM particle mass should be above ~ 150 GeV, for $\Gamma/M = 0.06$. In fermionic DM model, the factor $R_{q\bar{q}}$ is the same as R_{gg} in the scalar DM model. Thus the upper limit on the cross sections can be obtained from that in the scalar DM model by a rescaling factor $1/s_\chi = 1/4$.

For gg channel, using the best-fit values of m_χ and $\langle\sigma v\rangle_{gg}$ in Tab. 1, the corresponding minimal value of the width-to-mass ratio is found to be

$$\left(\frac{\Gamma}{M}\right)_{\text{fermion}, gg} \gtrsim 0.31 \left(\frac{M}{750 \text{ GeV}}\right)^3 \left(\frac{62 \text{ GeV}}{m_\chi}\right)^2 \left(\frac{\langle\sigma v\rangle_{gg}}{1.96 \times 10^{-26} \text{ cm}^3\text{s}^{-1}}\right)^{1/2}. \quad (31)$$

Such a large width is not favoured by the current experimental data and is theoretically unnatural.

For $q\bar{q}$ -channel, since $R_{q\bar{q}}$ is proportional to $(m_\chi/M)^4$, the required total width is similar to the case of gg -channel of scalar DM. For $b\bar{b}$ channel it is found that

$$\left(\frac{\Gamma}{M}\right)_{\text{fermion}, b\bar{b}} \gtrsim 0.058 \left(\frac{M}{750 \text{ GeV}}\right)^2 \left(\frac{46 \text{ GeV}}{m_\chi}\right) \left(\frac{\langle\sigma v\rangle_{gg}}{1.42 \times 10^{-26} \text{ cm}^3\text{s}^{-1}}\right)^{1/2}, \quad (32)$$

and the result is similar for the $c\bar{c}$ channel

$$\left(\frac{\Gamma}{M}\right)_{\text{fermion}, c\bar{c}} \gtrsim 0.062 \left(\frac{M}{750 \text{ GeV}}\right)^2 \left(\frac{35.5 \text{ GeV}}{m_\chi}\right) \left(\frac{\langle\sigma v\rangle_{gg}}{0.95 \times 10^{-26} \text{ cm}^3\text{s}^{-1}}\right)^{1/2}. \quad (33)$$

We perform χ^2 -fit to the diphoton and GCE data in the fermionic DM model for $b\bar{b}$ and $c\bar{c}$ channels with $\Gamma/M = 0.06$. The determined parameters are shown in Tab. 3, and the allowed regions of the parameters in $(\Gamma_{b\bar{b}}/M, \Gamma_{\gamma\gamma}/M)$ and $(\Gamma_{\chi\chi}/M, \Gamma_{\gamma\gamma}/M)$ planes are shown in Fig. 5. Compared with the same channel in the scalar DM model, a visible change in the allowed regions is that the regions corresponding to the two solutions merge together, which is due to the fact that in fermionic DM models, the value of Δ is quite small as the minimally required width is close to 0.06. The determined values of $\Gamma_{q\bar{q}}/M$ and $\Gamma_{\chi\chi}/M$ are roughly the same order of magnitude about $\mathcal{O}(10^{-2})$. The allowed regions are consistent with the Run-1 limit on cross section of the diphoton production.

Since in the fermionic DM model, $\Gamma_{\chi\chi}/M$ can reach $\mathcal{O}(10^{-2})$, it is expected that the predicted cross sections for the gamma-ray line are significantly larger than that in the scalar DM model. In Fig. 7, we show the predicted cross sections in this model for $b\bar{b}$ and $c\bar{c}$ channel with $\Gamma/M = 0.06$. The cross section can reach $\mathcal{O}(10^{-29}) \text{ cm}^3\text{s}^{-1}$, which is very close to the current Fermi-LAT limit, and can be tested in the future by Fermi-LAT, HESS and CTA.

In the case where χ is Dirac, the corresponding values of $R_{X\bar{X}}$ are the same. However, the required product of $(\Gamma_{\chi\bar{X}}/M)(\Gamma_{X\bar{X}}/M)$ increases by a factor of four from Eqs. (5) and

(12). Thus the required total width Γ/M is expected to be larger compared with all the cases of Majorana DM.

4.3 Vector DM

In the case where the DM particle is a Majorana fermion, the Lagrangian for DM and its interaction with ϕ is given by

$$\mathcal{L} \supset \frac{1}{4}\chi_{\mu\nu}\chi^{\mu\nu} - \frac{1}{2}m_\chi^2\chi_\mu\chi^\mu - \frac{1}{2}g_\chi\phi\chi_\mu\chi^\mu. \quad (34)$$

For $\chi\chi \rightarrow \phi \rightarrow gg, q\bar{q}$, the corresponding $R_{X\bar{X}}$ factors are given by

$$R_{gg} = \frac{192m_\chi^8}{M^8T(m_\chi/M)}, \quad R_{q\bar{q}} = \frac{64m_\chi^6\beta_q(4m_\chi^2)}{M^6\beta_q(M^2)T(m_\chi/M)}, \quad (35)$$

where $T(x) = 1 - 4x^2 + 12x^4$. Since in vector DM model $R_{gg} \propto (m_\chi/M)^8$ and $R_{q\bar{q}} \propto (m_\chi/M)^6$, it is expected that a very large Γ/M is required. For gg channel, the minimally required width is given by

$$\left(\frac{\Gamma}{M}\right)_{\text{vector}, gg} \gtrsim 3.3 \left(\frac{M}{750 \text{ GeV}}\right)^4 \left(\frac{62 \text{ GeV}}{m_\chi}\right)^3 \left(\frac{\langle\sigma v\rangle_{gg}}{1.96 \times 10^{-26} \text{ cm}^3\text{s}^{-1}}\right)^{1/2}, \quad (36)$$

and for $q\bar{q}$ channel

$$\left(\frac{\Gamma}{M}\right)_{\text{fermion}, b\bar{b}} \gtrsim 0.73 \left(\frac{M}{750 \text{ GeV}}\right)^3 \left(\frac{46 \text{ GeV}}{m_\chi}\right)^2 \left(\frac{\langle\sigma v\rangle_{gg}}{1.42 \times 10^{-26} \text{ cm}^3\text{s}^{-1}}\right)^{1/2}. \quad (37)$$

The results for the $c\bar{c}$ channel is similar to that in the $b\bar{b}$ channel. Thus in all the cases, the required ϕ width are too large and already ruled out by the current Run-2 data, which indicates that the vector DM model can not provide a consistent explanation to the LHC Run-2 diphoton excess and the GCE.

5 Conclusions

In summary, we have investigate the conditions for a consistent explanation for possible the LHC diphoton excess and GCE, especially the requirement on total width of ϕ in a wide range of DM models where the DM particle can be scalar, fermionionic and vector, and ϕ can be generated by s -channel gluon fusion or quark-antiquark annihilation ($b\bar{b}$ and $c\bar{c}$) at parton level. We have shown that the required Γ/M is determined by a single parameter proportional to $(m_\chi/M)^n$. We have found that three models can explain the two excesses successfully: i) scalar DM model with ϕ coupling dominantly with $q\bar{q}$. the minimally required Γ/M can be as low as $\mathcal{O}(10^{-3})$; ii) scalar DM model with ϕ coupling

dominantly with gg , the required Γ/M is about $\mathcal{O}(10^{-2})$; iii) fermionic DM model with coupling dominantly with $q\bar{q}$, the required Γ/M reaches $\mathcal{O}(10^{-2})$. Other models such as the vector DM model requires larger Γ/M of order one which is already disfavoured by the current data. For the same DM model, the required width of ϕ is always smaller in $q\bar{q}$ channel than that in the gg channel. For the DM models which can simultaneously account for the diphoton excess and the GCE, the predicted cross sections for gamma-ray line are typically of $\mathcal{O}(10^{-30}) \text{ cm}^3\text{s}^{-1}$, which is close to the current limits imposed by the Fermi-LAT data. These models can be distinguish soon by the updated LHC data, through the measurement of the total width, and Fermi-LAT data on the gamma-ray line searches in the near future.

Acknowledgements. This work is supported by the NSFC under Grants No. 11335012 and No. 11475237.

References

- [1] LHC seminar, ATLAS and CMS physics results from Run 2, talks by Jim Olsen and Marumi Kado, CERN, 15 Dec. 2015. ATLAS note, ATLAS-CONF-2015-081, CMS note, CMS PAS EXO- 15-004.
- [2] CMS Collaboration, CMS-EXO-16-018.
- [3] L.D. Landau, Dokl.Akad.Nauk.Ser.Fiz. 60(1948)2,207; C.N.Yang, Phys.Rev.D77,242.
- [4] R. Franceschini, G. F. Giudice, J. F. Kamenik, M. McCullough, A. Pomarol, R. Rattazzi, M. Redi, F. Riva, A. Strumia, and R. Torre, *What is the $\gamma\gamma$ resonance at 750 GeV?*, *JHEP* **03** (2016) 144, [[arXiv:1512.04933](#)].
- [5] D. Buttazzo, A. Greljo, and D. Marzocca, *Knocking on new physics door with a scalar resonance*, *Eur. Phys. J.* **C76** (2016), no. 3 116, [[arXiv:1512.04929](#)].
- [6] A. Falkowski, O. Slone, and T. Volansky, *Phenomenology of a 750 GeV Singlet*, *JHEP* **02** (2016) 152, [[arXiv:1512.05777](#)].
- [7] M. Low, A. Tesi, and L.-T. Wang, *A pseudoscalar decaying to photon pairs in the early LHC Run 2 data*, *JHEP* **03** (2016) 108, [[arXiv:1512.05328](#)].
- [8] P. Agrawal, J. Fan, B. Heidenreich, M. Reece, and M. Strassler, *Experimental Considerations Motivated by the Diphoton Excess at the LHC*, [arXiv:1512.05775](#).
- [9] Y. Mambrini, G. Arcadi, and A. Djouadi, *The LHC diphoton resonance and dark matter*, *Phys. Lett.* **B755** (2016) 426–432, [[arXiv:1512.04913](#)].

- [10] M. Backovic, A. Mariotti, and D. Redigolo, *Di-photon excess illuminates Dark Matter*, *JHEP* **03** (2016) 157, [[arXiv:1512.04917](#)].
- [11] X.-J. Bi, Q.-F. Xiang, P.-F. Yin, and Z.-H. Yu, *The 750 GeV diphoton excess at the LHC and dark matter constraints*, *Nucl. Phys.* **B909** (2016) 43–64, [[arXiv:1512.06787](#)].
- [12] D. Barducci, A. Goudelis, S. Kulkarni, and D. Sengupta, *One jet to rule them all: monojet constraints and invisible decays of a 750 GeV diphoton resonance*, [arXiv:1512.06842](#).
- [13] Y. Bai, J. Berger, and R. Lu, *750 GeV dark pion: Cousin of a dark G -parity odd WIMP*, *Phys. Rev.* **D93** (2016), no. 7 076009, [[arXiv:1512.05779](#)].
- [14] C. Han, H. M. Lee, M. Park, and V. Sanz, *The diphoton resonance as a gravity mediator of dark matter*, *Phys. Lett.* **B755** (2016) 371–379, [[arXiv:1512.06376](#)].
- [15] M. Bauer and M. Neubert, *Flavor Anomalies, the Diphoton Excess and a Dark Matter Candidate*, [arXiv:1512.06828](#).
- [16] P. S. B. Dev and D. Teresi, *Asymmetric Dark Matter in the Sun and the Diphoton Excess at the LHC*, [arXiv:1512.07243](#).
- [17] H. Davoudiasl and C. Zhang, *750 GeV messenger of dark conformal symmetry breaking*, *Phys. Rev.* **D93** (2016), no. 5 055006, [[arXiv:1512.07672](#)].
- [18] F. D’Eramo, J. de Vries, and P. Panci, *A 750 GeV Portal: LHC Phenomenology and Dark Matter Candidates*, *JHEP* **05** (2016) 089, [[arXiv:1601.01571](#)].
- [19] X. Chu, T. Hambye, T. Scarna, and M. H. G. Tytgat, *What if Dark Matter Gamma-Ray Lines come with Gluon Lines?*, *Phys. Rev.* **D86** (2012) 083521, [[arXiv:1206.2279](#)].
- [20] J.-C. Park and S. C. Park, *Indirect signature of dark matter with the diphoton resonance at 750 GeV*, [arXiv:1512.08117](#).
- [21] L. Goodenough and D. Hooper, *Possible Evidence For Dark Matter Annihilation In The Inner Milky Way From The Fermi Gamma Ray Space Telescope*, [arXiv:0910.2998](#).
- [22] D. Hooper and L. Goodenough, *Dark Matter Annihilation in The Galactic Center As Seen by the Fermi Gamma Ray Space Telescope*, *Phys. Lett.* **B697** (2011) 412–428, [[arXiv:1010.2752](#)].

- [23] A. Boyarsky, D. Malyshev, and O. Ruchayskiy, *A comment on the emission from the Galactic Center as seen by the Fermi telescope*, *Phys. Lett.* **B705** (2011) 165–169, [[arXiv:1012.5839](#)].
- [24] K. N. Abazajian, *The Consistency of Fermi-LAT Observations of the Galactic Center with a Millisecond Pulsar Population in the Central Stellar Cluster*, *JCAP* **1103** (2011) 010, [[arXiv:1011.4275](#)].
- [25] D. Hooper and T. Linden, *On The Origin Of The Gamma Rays From The Galactic Center*, *Phys. Rev.* **D84** (2011) 123005, [[arXiv:1110.0006](#)].
- [26] K. N. Abazajian and M. Kaplinghat, *Detection of a Gamma-Ray Source in the Galactic Center Consistent with Extended Emission from Dark Matter Annihilation and Concentrated Astrophysical Emission*, *Phys. Rev.* **D86** (2012) 083511, [[arXiv:1207.6047](#)]. [Erratum: *Phys. Rev.* D87,129902(2013)].
- [27] C. Gordon and O. Macias, *Dark Matter and Pulsar Model Constraints from Galactic Center Fermi-LAT Gamma Ray Observations*, *Phys. Rev.* **D88** (2013), no. 8 083521, [[arXiv:1306.5725](#)]. [Erratum: *Phys. Rev.* D89,no.4,049901(2014)].
- [28] O. Macias and C. Gordon, *Contribution of cosmic rays interacting with molecular clouds to the Galactic Center gamma-ray excess*, *Phys. Rev.* **D89** (2014), no. 6 063515, [[arXiv:1312.6671](#)].
- [29] K. N. Abazajian, N. Canac, S. Horiuchi, and M. Kaplinghat, *Astrophysical and Dark Matter Interpretations of Extended Gamma-Ray Emission from the Galactic Center*, *Phys. Rev.* **D90** (2014), no. 2 023526, [[arXiv:1402.4090](#)].
- [30] D. Hooper and T. R. Slatyer, *Two Emission Mechanisms in the Fermi Bubbles: A Possible Signal of Annihilating Dark Matter*, *Phys. Dark Univ.* **2** (2013) 118–138, [[arXiv:1302.6589](#)].
- [31] W.-C. Huang, A. Urbano, and W. Xue, *Fermi Bubbles under Dark Matter Scrutiny. Part I: Astrophysical Analysis*, [arXiv:1307.6862](#).
- [32] T. Daylan, D. P. Finkbeiner, D. Hooper, T. Linden, S. K. N. Portillo, N. L. Rodd, and T. R. Slatyer, *The characterization of the gamma-ray signal from the central Milky Way: A case for annihilating dark matter*, *Phys. Dark Univ.* **12** (2016) 1–23, [[arXiv:1402.6703](#)].
- [33] B. Zhou, Y.-F. Liang, X. Huang, X. Li, Y.-Z. Fan, L. Feng, and J. Chang, *GeV excess in the Milky Way: The role of diffuse galactic gamma-ray emission templates*, *Phys. Rev.* **D91** (2015), no. 12 123010, [[arXiv:1406.6948](#)].

- [34] F. Calore, I. Cholis, and C. Weniger, *Background model systematics for the Fermi GeV excess*, *JCAP* **1503** (2015) 038, [[arXiv:1409.0042](#)].
- [35] **Fermi-LAT** Collaboration, M. Ajello et al., *Fermi-LAT Observations of High-Energy γ -Ray Emission Toward the Galactic Center*, *Astrophys. J.* **819** (2016), no. 1 44, [[arXiv:1511.02938](#)].
- [36] R. Bartels, S. Krishnamurthy, and C. Weniger, *Strong support for the millisecond pulsar origin of the Galactic center GeV excess*, *Phys. Rev. Lett.* **116** (2016), no. 5 051102, [[arXiv:1506.05104](#)].
- [37] S. K. Lee, M. Lisanti, B. R. Safdi, T. R. Slatyer, and W. Xue, *Evidence for Unresolved γ -Ray Point Sources in the Inner Galaxy*, *Phys. Rev. Lett.* **116** (2016), no. 5 051103, [[arXiv:1506.05124](#)].
- [38] D. Gaggero, M. Taoso, A. Urbano, M. Valli, and P. Ullio, *Towards a realistic astrophysical interpretation of the gamma-ray Galactic center excess*, *JCAP* **1512** (2015), no. 12 056, [[arXiv:1507.06129](#)].
- [39] P. Agrawal, B. Batell, P. J. Fox, and R. Harnik, *WIMPs at the Galactic Center*, *JCAP* **1505** (2015) 011, [[arXiv:1411.2592](#)].
- [40] X.-J. Huang, W.-H. Zhang, and Y.-F. Zhou, *A 750 GeV dark matter messenger at the Galactic Center*, [arXiv:1512.08992](#).
- [41] A. Hektor and L. Marzola, *Di-photon excess at LHC and the gamma ray excess at the Galactic Centre*, [arXiv:1602.00004](#).
- [42] M. E. Krauss, T. Opferkuch, F. Staub, and M. W. Winkler, *The 750 GeV Boson: Dawn of the Super-Hooperon*, [arXiv:1605.05327](#).
- [43] **ATLAS** Collaboration, G. Aad et al., *Search for new resonances in $W\gamma$ and $Z\gamma$ final states in pp collisions at $\sqrt{s} = 8$ TeV with the ATLAS detector*, *Phys. Lett. B* **738** (2014) 428–447, [[arXiv:1407.8150](#)].
- [44] **ATLAS** Collaboration, G. Aad et al., *Search for an additional, heavy Higgs boson in the $H \rightarrow ZZ$ decay channel at $\sqrt{s} = 8$ TeV in pp collision data with the ATLAS detector*, *Eur. Phys. J.* **C76** (2016), no. 1 45, [[arXiv:1507.05930](#)].
- [45] **CMS** Collaboration, V. Khachatryan et al., *Search for a Higgs Boson in the Mass Range from 145 to 1000 GeV Decaying to a Pair of W or Z Bosons*, *JHEP* **10** (2015) 144, [[arXiv:1504.00936](#)].

- [46] **ATLAS** Collaboration, G. Aad et al., *Search for a high-mass Higgs boson decaying to a W boson pair in pp collisions at $\sqrt{s} = 8$ TeV with the ATLAS detector*, *JHEP* **01** (2016) 032, [[arXiv:1509.00389](#)].
- [47] **ATLAS** Collaboration, G. Aad et al., *Search for high-mass diphoton resonances in pp collisions at $\sqrt{s} = 8$ TeV with the ATLAS detector*, *Phys. Rev.* **D92** (2015), no. 3 032004, [[arXiv:1504.05511](#)].
- [48] **ATLAS** Collaboration, G. Aad et al., *Search for new phenomena in the dijet mass distribution using $p - p$ collision data at $\sqrt{s} = 8$ TeV with the ATLAS detector*, *Phys. Rev.* **D91** (2015), no. 5 052007, [[arXiv:1407.1376](#)].
- [49] **CMS** Collaboration, V. Khachatryan et al., *Search for neutral MSSM Higgs bosons decaying into a pair of bottom quarks*, *JHEP* **11** (2015) 071, [[arXiv:1506.08329](#)].
- [50] J. F. Navarro, C. S. Frenk, and S. D. M. White, *A Universal density profile from hierarchical clustering*, *Astrophys. J.* **490** (1997) 493–508, [[astro-ph/9611107](#)].
- [51] T. Sjostrand, S. Mrenna, and P. Z. Skands, *A Brief Introduction to PYTHIA 8.1*, *Comput. Phys. Commun.* **178** (2008) 852–867, [[arXiv:0710.3820](#)].
- [52] F. Calore, I. Cholis, C. McCabe, and C. Weniger, *A Tale of Tails: Dark Matter Interpretations of the Fermi GeV Excess in Light of Background Model Systematics*, *Phys. Rev.* **D91** (2015), no. 6 063003, [[arXiv:1411.4647](#)].
- [53] **Fermi-LAT** Collaboration, M. Ackermann et al., *Searching for Dark Matter Annihilation from Milky Way Dwarf Spheroidal Galaxies with Six Years of Fermi Large Area Telescope Data*, *Phys. Rev. Lett.* **115** (2015), no. 23 231301, [[arXiv:1503.02641](#)].
- [54] P. Ullio and M. Valli, *A critical reassessment of particle Dark Matter limits from dwarf satellites*, [arXiv:1603.07721](#).
- [55] H.-B. Jin, Y.-L. Wu, and Y.-F. Zhou, *Upper limits on dark matter annihilation cross sections from the first AMS-02 antiproton data*, *Phys. Rev.* **D92** (2015), no. 5 055027, [[arXiv:1504.04604](#)].
- [56] H.-B. Jin, Y.-L. Wu, and Y.-F. Zhou, *Implications of the first AMS-02 antiproton data for dark matter*, *Int. J. Mod. Phys.* **A30** (2015), no. 28n29 1545008, [[arXiv:1508.06844](#)].

- [57] D. Hooper, T. Linden, and P. Mertsch, *What Does The PAMELA Antiproton Spectrum Tell Us About Dark Matter?*, *JCAP* **1503** (2015), no. 03 021, [[arXiv:1410.1527](#)].
- [58] H.-B. Jin, S. Miao, and Y.-F. Zhou, *Implications of the latest XENON100 and cosmic ray antiproton data for isospin violating dark matter*, *Phys. Rev.* **D87** (2013), no. 1 016012, [[arXiv:1207.4408](#)].
- [59] H.-B. Jin, Y.-L. Wu, and Y.-F. Zhou, *Cosmic ray propagation and dark matter in light of the latest AMS-02 data*, *JCAP* **1509** (2015), no. 09 049, [[arXiv:1410.0171](#)].
- [60] H.-B. Jin, Y.-L. Wu, and Y.-F. Zhou, *Implications of the first AMS-02 measurement for dark matter annihilation and decay*, *JCAP* **1311** (2013) 026, [[arXiv:1304.1997](#)].
- [61] A. Ibarra, A. S. Lamperstorfer, and J. Silk, *Dark matter annihilations and decays after the AMS-02 positron measurements*, *Phys. Rev.* **D89** (2014), no. 6 063539, [[arXiv:1309.2570](#)].
- [62] R. D. Peccei and H. R. Quinn, *Phys. Rev. D* **16**, 1791 (1977); R. D. Peccei and H. R. Quinn, *Phys. Rev. Lett.* **38**, 1440 (1977); J. E. Kim, *Phys. Rept.* **150**, 1 (1987).
- [63] B. Gripaios, A. Pomarol, F. Riva, and J. Serra, *Beyond the Minimal Composite Higgs Model*, *JHEP* **04** (2009) 070, [[arXiv:0902.1483](#)].
- [64] A. Angelescu, A. Djouadi, and G. Moreau, *Scenarii for interpretations of the LHC diphoton excess: two Higgs doublets and vector-like quarks and leptons*, *Phys. Lett.* **B756** (2016) 126–132, [[arXiv:1512.04921](#)].
- [65] X.-F. Han and L. Wang, *Implication of the 750 GeV diphoton resonance on two-Higgs-doublet model and its extensions with Higgs field*, *Phys. Rev.* **D93** (2016), no. 5 055027, [[arXiv:1512.06587](#)].
- [66] W.-C. Huang, Y.-L. S. Tsai, and T.-C. Yuan, *Gauged Two Higgs Doublet Model confronts the LHC 750 GeV diphoton anomaly*, *Nucl. Phys.* **B909** (2016) 122–134, [[arXiv:1512.07268](#)].
- [67] S. Moretti and K. Yagyu, *750 GeV diphoton excess and its explanation in two-Higgs-doublet models with a real inert scalar multiplet*, *Phys. Rev.* **D93** (2016), no. 5 055043, [[arXiv:1512.07462](#)].
- [68] M. Badziak, *Interpreting the 750 GeV diphoton excess in minimal extensions of Two-Higgs-Doublet models*, [arXiv:1512.07497](#).

- [69] X.-F. Han, L. Wang, L. Wu, J. M. Yang, and M. Zhang, *Explaining 750 GeV diphoton excess from top/bottom partner cascade decay in two-Higgs-doublet model extension*, *Phys. Lett.* **B756** (2016) 309–316, [[arXiv:1601.00534](#)].
- [70] X.-F. Han, L. Wang, and J. M. Yang, *An extension of two-Higgs-doublet model and the excesses of 750 GeV diphoton, muon $g-2$ and $h \rightarrow \mu\tau$* , *Phys. Lett.* **B757** (2016) 537–547, [[arXiv:1601.04954](#)].
- [71] S. Gopalakrishna and T. S. Mukherjee, *The 750 GeV diphoton excess in a two Higgs doublet model and a singlet scalar model, with vector-like fermions, unitarity constraints, and dark matter implications*, [arXiv:1604.05774](#).
- [72] S.-F. Ge, H.-J. He, J. Ren, and Z.-Z. Xianyu, *Realizing Dark Matter and Higgs Inflation in Light of LHC Diphoton Excess*, *Phys. Lett.* **B757** (2016) 480–492, [[arXiv:1602.01801](#)].
- [73] U. K. Dey, S. Mohanty, and G. Tomar, *750 GeV resonance in the dark leftright model*, *Phys. Lett.* **B756** (2016) 384–389, [[arXiv:1512.07212](#)].
- [74] A. Dasgupta, M. Mitra, and D. Borah, *Minimal Left-Right Symmetry Confronted with the 750 GeV Di-photon Excess at LHC*, [arXiv:1512.09202](#).
- [75] D. Borah, S. Patra, and S. Sahoo, *Subdominant Left-Right Scalar Dark Matter as Origin of the 750 GeV Di-photon Excess at LHC*, [arXiv:1601.01828](#).
- [76] D. T. Huong and P. V. Dong, *Left-right asymmetry and 750 GeV diphoton excess*, *Phys. Rev.* **D93** (2016) 095019, [[arXiv:1603.05146](#)].
- [77] P. S. B. Dev, R. N. Mohapatra, and Y. Zhang, *Quark Seesaw, Vectorlike Fermions and Diphoton Excess*, *JHEP* **02** (2016) 186, [[arXiv:1512.08507](#)].
- [78] W.-L. Guo, Y.-L. Wu, and Y.-F. Zhou, *Dark matter candidates in left-right symmetric models*, *Int. J. Mod. Phys.* **D20** (2011) 1389–1397.
- [79] W.-L. Guo, Y.-L. Wu, and Y.-F. Zhou, *Searching for Dark Matter Signals in the Left-Right Symmetric Gauge Model with CP Symmetry*, *Phys. Rev.* **D82** (2010) 095004, [[arXiv:1008.4479](#)].
- [80] W.-L. Guo, Y.-L. Wu, and Y.-F. Zhou, *Exploration of decaying dark matter in a left-right symmetric model*, *Phys. Rev.* **D81** (2010) 075014, [[arXiv:1001.0307](#)].
- [81] W.-L. Guo, L.-M. Wang, Y.-L. Wu, Y.-F. Zhou, and C. Zhuang, *Gauge-singlet dark matter in a left-right symmetric model with spontaneous CP violation*, *Phys. Rev.* **D79** (2009) 055015, [[arXiv:0811.2556](#)].

- [82] Y.-L. Wu and Y.-F. Zhou, *Two Higgs Bi-doublet Left-Right Model With Spontaneous P and CP Violation*, *Sci. China* **G51** (2008) 1808–1825, [[arXiv:0709.0042](#)].
- [83] J. Ellis, S. A. R. Ellis, J. Quevillon, V. Sanz, and T. You, *On the Interpretation of a Possible ~ 750 GeV Particle Decaying into $\gamma\gamma$* , *JHEP* **03** (2016) 176, [[arXiv:1512.05327](#)].
- [84] L. Bian, N. Chen, D. Liu and J. Shu, [arXiv:1512.05759](#); W. Liao and H. q. Zheng, [arXiv:1512.06741](#); R. Ding, L. Huang, T. Li and B. Zhu, [arXiv:1512.06560](#); M. x. Luo, K. Wang, T. Xu, L. Zhang and G. Zhu, [arXiv:1512.06670](#); T. F. Feng, X. Q. Li, H. B. Zhang and S. M. Zhao, [arXiv:1512.06696](#); F. Wang, L. Wu, J. M. Yang and M. Zhang, [arXiv:1512.06715](#); X. F. Han and L. Wang, [arXiv:1512.06587](#); W. C. Huang, Y. L. S. Tsai and T. C. Yuan, [arXiv:1512.07268](#); J. Cao, C. Han, L. Shang, W. Su, J. M. Yang and Y. Zhang, [arXiv:1512.06728](#); Q. H. Cao, Y. Liu, K. P. Xie, B. Yan and D. M. Zhang, [arXiv:1512.05542](#); Q. H. Cao, Y. Liu, K. P. Xie, B. Yan and D. M. Zhang, [arXiv:1512.08441](#); B. C. Allanach, P. S. B. Dev, S. A. Renner and K. Sakurai, [arXiv:1512.07645](#).
- [85] **Fermi-LAT** Collaboration, M. Ackermann et al., *Updated search for spectral lines from Galactic dark matter interactions with pass 8 data from the Fermi Large Area Telescope*, *Phys. Rev.* **D91** (2015), no. 12 122002, [[arXiv:1506.00013](#)].

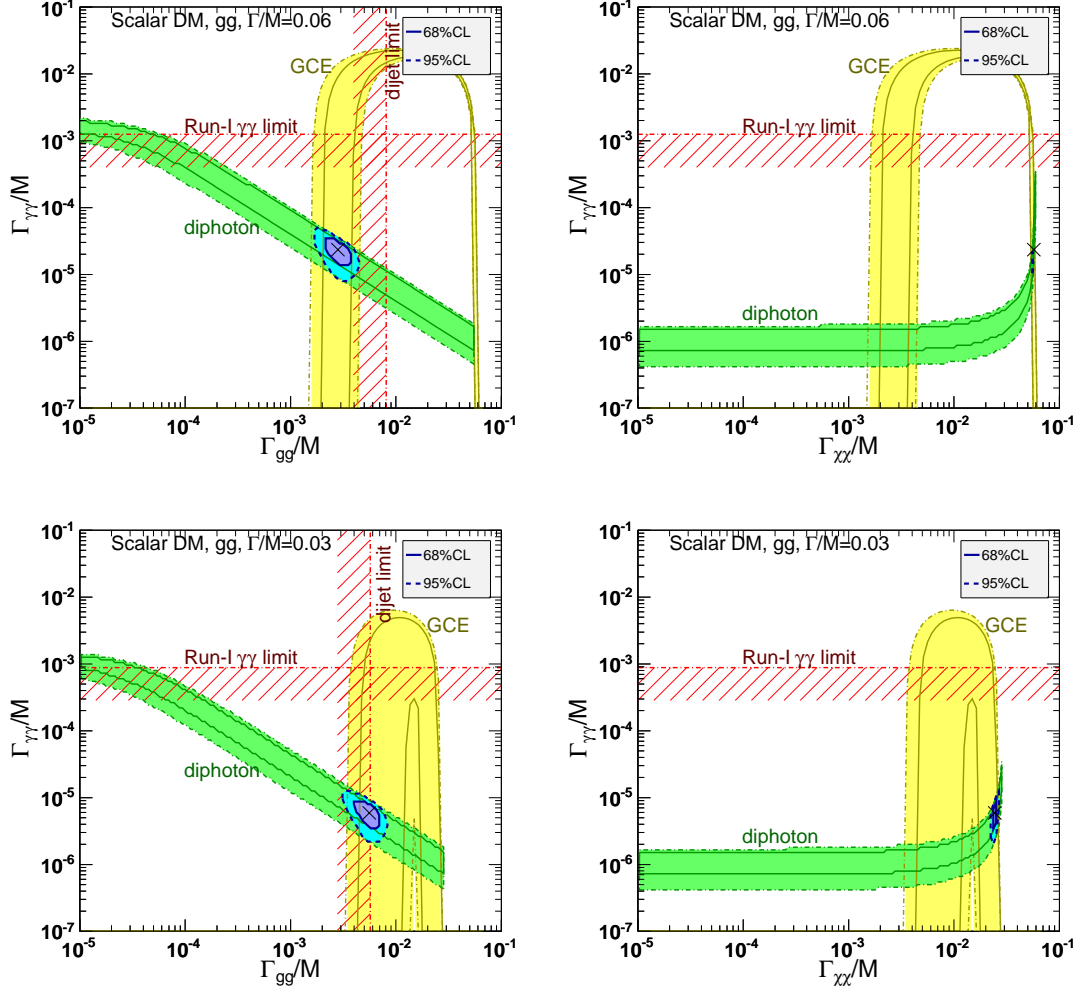


FIG. 2: Upper panels) Left: Allowed regions at 60% and 95% C.L. in $(\Gamma_{gg}/M, \Gamma_{\gamma\gamma}/M)$ plane from a combined fit to both the LHC diphoton excess and the GCE in a scalar DM model with gg fusion, together with the regions allowed by each individual experiment. The upper limits from Run-1 on the dijet and diphoton production cross sections are also shown. The total width is fixed at $\Gamma/M = 0.06$. Right: The same as upper-left, but in $(\Gamma_{\chi\chi}/M, \Gamma_{\gamma\gamma}/M)$ plane. Lower panels) The same as upper pannels but for $\Gamma/M = 0.03$.

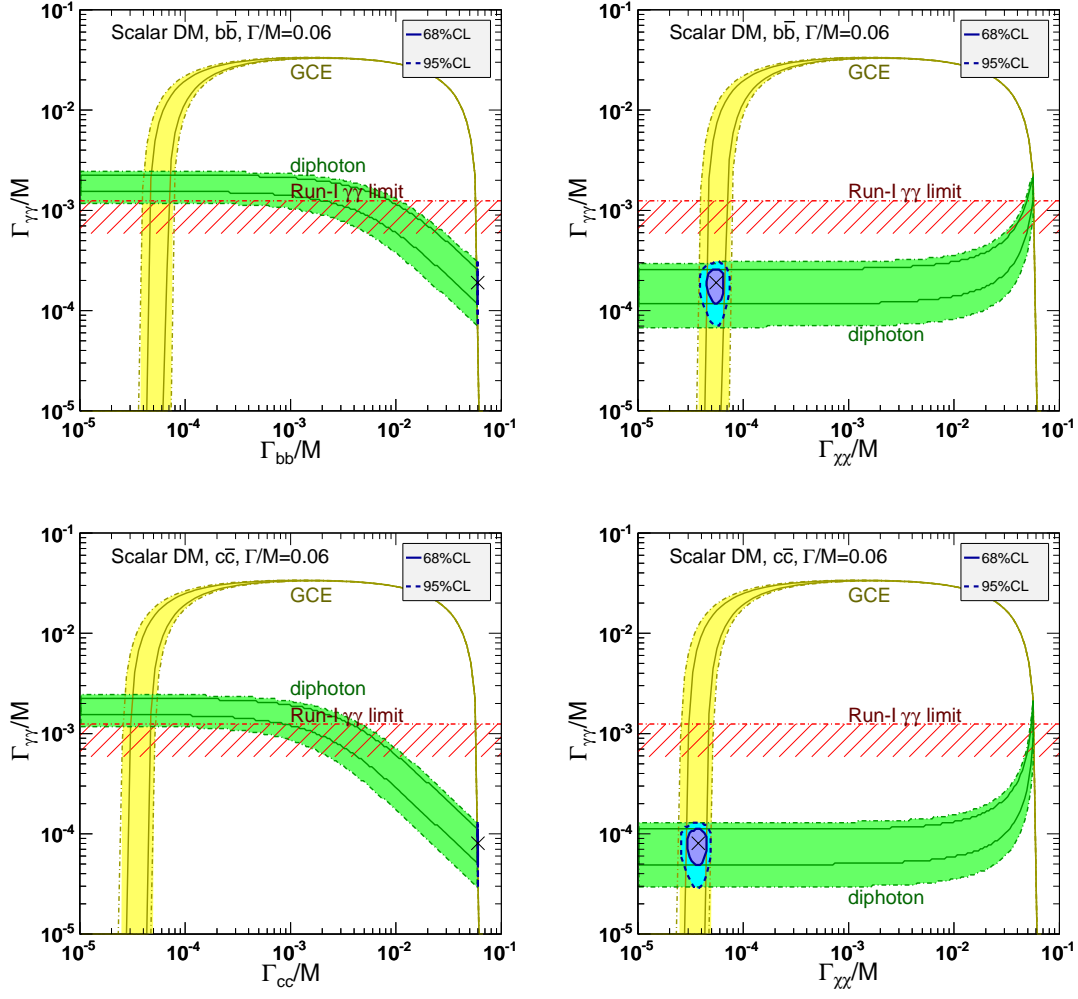


FIG. 3: The same as Fig. 2, but for scalar DM models with ϕ generated from $b\bar{b}$ (upper panels) and $c\bar{c}$ (lower panels) annihilation at the LHC for $\Gamma/M = 0.06$.

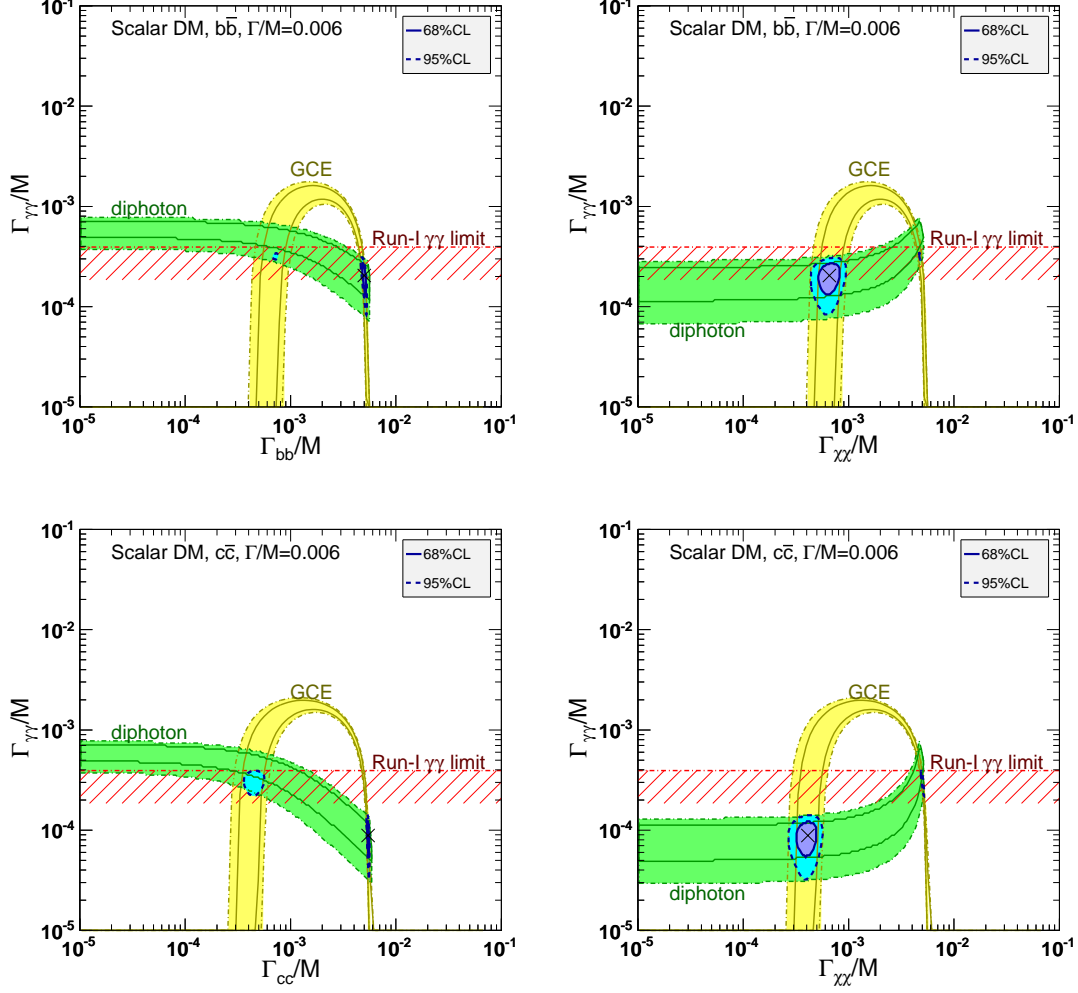


FIG. 4: The same as Fig. 3, but for $\Gamma/M = 0.006$.

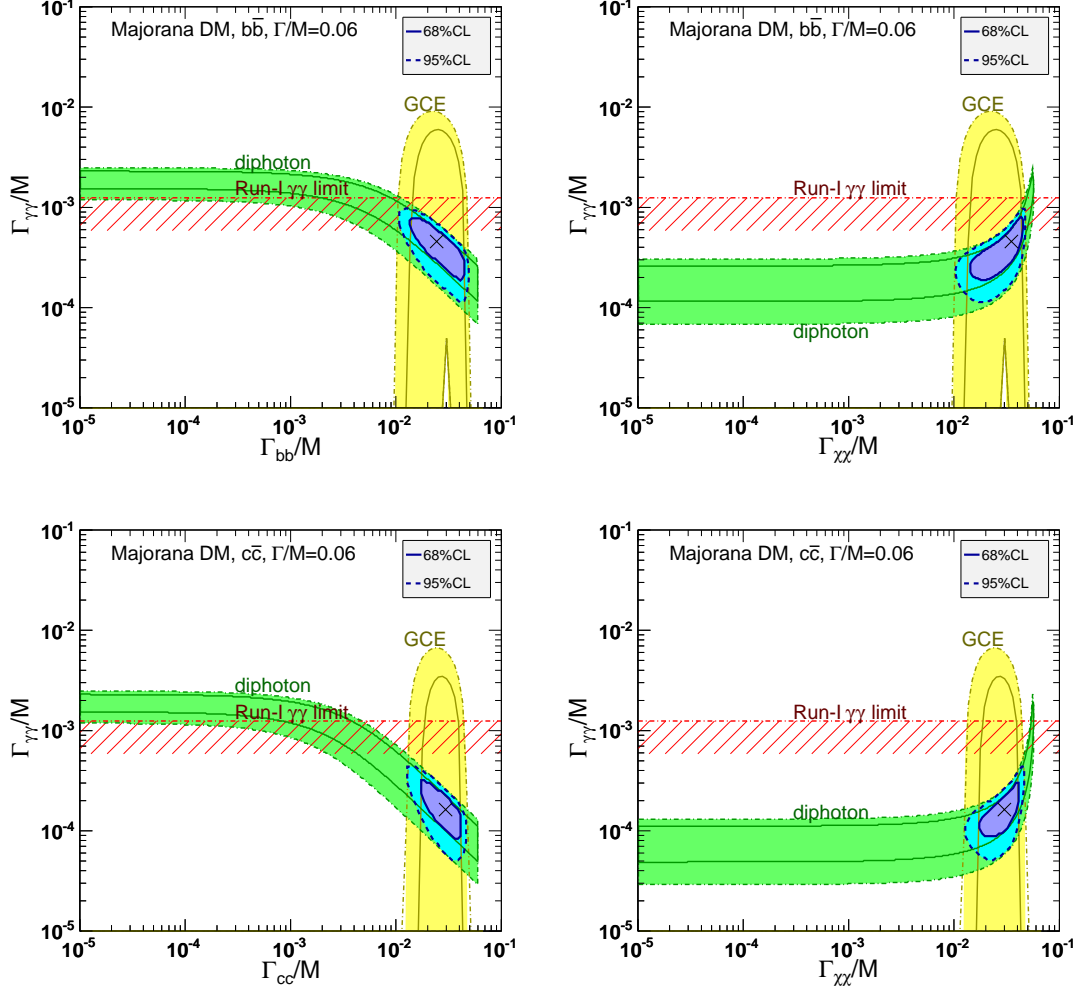


FIG. 5: The same as Fig. 3 but for the Majorana fermionic DM model.

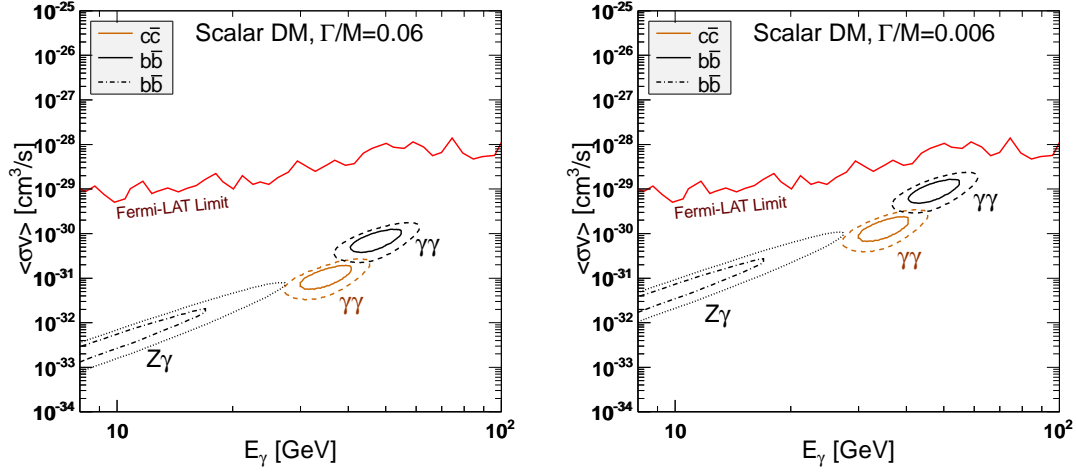


FIG. 6: Left) Predictions for $\langle\sigma v\rangle_{\gamma\gamma}$ and $\langle\sigma v\rangle_{Z\gamma}$ as a function of photon energy in the scalar DM model with ϕ coupling dominantly with $b\bar{b}$ and $c\bar{c}$, using the allowed parameters from the fit to the data of diphoton excess and GCE, for $\Gamma/M = 0.06$. The exclusion limits at 95% C.L. of Fermi-LAT [85] for region R16 are also shown.

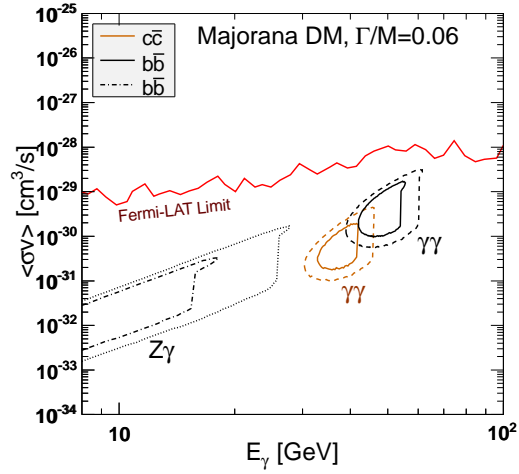


FIG. 7: The same as Fig. 6, but for Majorana DM model and $\Gamma/M = 0.06$.